5-2013

Improvements in Microdialysis Sampling Extraction Efficiency Using Recycled Flow

Justin Cole Deaton
University of Arkansas, Fayetteville

Improvements in Microdialysis Sampling Extraction Efficiency Using Recycled Flow

Improvements in Microdialysis Sampling Extraction Efficiency Using Recycled Flow

A thesis submitted in partial fulfillment
of the requirements for the degree of
Master of Science in Microelectronics-Photonics

By

Justin Cole Deaton
Henderson State University
Bachelor of Science in Physics, 2008

May 2013
University of Arkansas

Abstract

Incomplete recovery during microdialysis sampling is hindering important research in neurology, proteomics, and immunology. Although the current generalized solution, decreasing volumetric flow rates (Q), has been and will remain to be a useful strategy it has reached it's a physical limitation due to evaporation at the collection site. Consequently, many important signaling molecules, such as signaling proteins, remain difficult to study. It is more fundamental to consider relative recovery as a function of the interaction time between the perfusate and the environment surrounding the probe.

In this work an increase in relative recovery was predicted by a mathematical model. Using recycled flow and flow reversal an increase in extraction efficiency was achieved at constant Q. It was observed that the recovery increase decrease as the number of passes increase.

This thesis is approved for recommendation to the Graduate Council.

Thesis Director:

_____
Prof. Ken Vickers

Thesis Committee:

_____
Dr. David Paul

_____
Dr. Rick Ulrich

The following signatories attest that all software used in this thesis was legally licensed for use by Mr. Ken Vickers for research purposes and publication.

_____ _____
Mr. Justin Cole Deaton Mr. Ken Vickers

This thesis was submitted to http://www.turnitin.com for plagiarism review by the TurnItIn's software. The signatory has examined the report on this thesis that was returned by TurnItIn and attest that, in his opinion, the items highlighted by the software are incidental to common usage and are not plagiarized material.

_____
Mr. Ken Vickers, Program Director

Thesis Duplication Release

I hereby authorize the University of Arkansas Libraries to duplicate this thesis when needed for research and/or scholarship.

Agreed_____
Justin Cole Deaton

Refused_____
Justin Cole Deaton

Acknowledgements

I would like to thank Jesus, my momma, and Ken Vickers for being with me in my hour of darkness.

I would like to acknowledge Dr. Julie Stenken. Dr. Stenken for provided me with a problem to work on, guidance in how to approach that problem, and a laboratory to work in. This work would not have been possible without her support, laboratory, equipment and instrumentation.

This thesis is based upon work supported by the National Science Foundation under Grant No. NSF EB-001441. Any opinions, findings, and conclusions or recommendations expressed in this material are those of the author(s) and do not necessarily reflect the views of the National Science Foundation.

Research reported in this thesis was supported by [the National Institutes of Health under grant number NIH NS-075874. The content is solely the responsibility of the authors and does not necessarily represent the official views of the National Institutes of Health.

Contents

Chapter 1: Introduction

1.1 Overview and Origins of Traditional Microdialysis Sampling

Mammalian cells communicate with one another by sending and receiving molecules across the extracellular space that separates them. On a local level this extracellular space possesses the properties of a fluid and is commonly referred to as the extracellular fluid (ECF) [1]. To fully understand the process of cell communication researchers must be able to describe a three variable system consisting of the concentration distribution of all the molecules that exist in the ECF in space and time.

Microdialysis sampling is a technique commonly used in life science research to extract (or collect) molecules that exist in the ECF within living tissues [2]. Microdialysis sampling collections, when paired with suitable analytical chemistry instrumentation, allows researchers to gain information on how the molecular concentrations change over time within the ECF of biological tissues [3].

The first time the word microdialysis can be found in literature is 1958. Kalant used the word to describe the simultaneous extraction and dialysis of steroids in the blood [4]. The precursor to microdialysis sampling was a push–pull perfusion device that was used to study mammalian brain chemistry. These push–pull perfusion devices were used to collect fluid relevant to synaptic transmission.

Perfusion fluid could be pumped into a small membranous sack that was inserted into a specific portion in the brain. After a period of time the fluid would be removed from the sack by a pump and analyzed to see what molecules had diffused into the fluid. Microdialysis is similar

to push-pull because both methods require the implantation of a small object in the tissue. However, microdialysis sampling was superior because it allowed finer temporal resolution of the ECF concentrations being studied, because the fluid was allowed to flow through the probe. Microdialysis sampling, as it is known today, did not appear until 1974, when it was used to monitor neurotransmitters in rat brain [5].

1.2 Microdialysis Probes: CMA 20

Figure 1 is a picture of a CMA 20 microdialysis probe. This picture was taken from the CMA Microdialysis product catalog [6]. The membrane is the white portion at the end of the probe. There are two possible membrane materials either polyarylethersulphone (PAES) or polyethersulphone (PES). The effective difference between the two membranes is that the PAES membrane has a 20kDa molecular weight (MW) cutoff and the PES membrane has a 100kDa cutoff. The upper portion of the shaft and the inner cannula is made of polyurethane, and is therefore flexible.

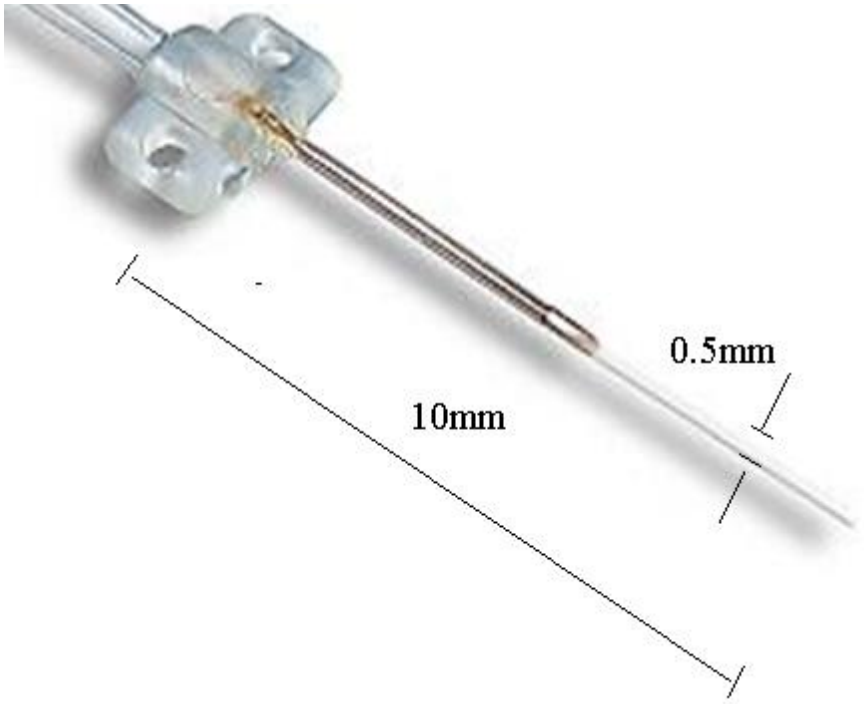

Figure 1 is a picture of a CMA 20 microdialysis sampling probe, taken from the CMA catalogue with dimensions added [6].

Figure 2 is a picture of the CMA 12 microdialysis probe. This picture was taken from the CMA Microdialysis product catalog [6]. The membrane is the white portion at the end of the probe. The membrane material is polyarylethersulphone (PAES) (20kDa MW cutoff). The upper portion of the shaft is steel, and is therefore inflexible.

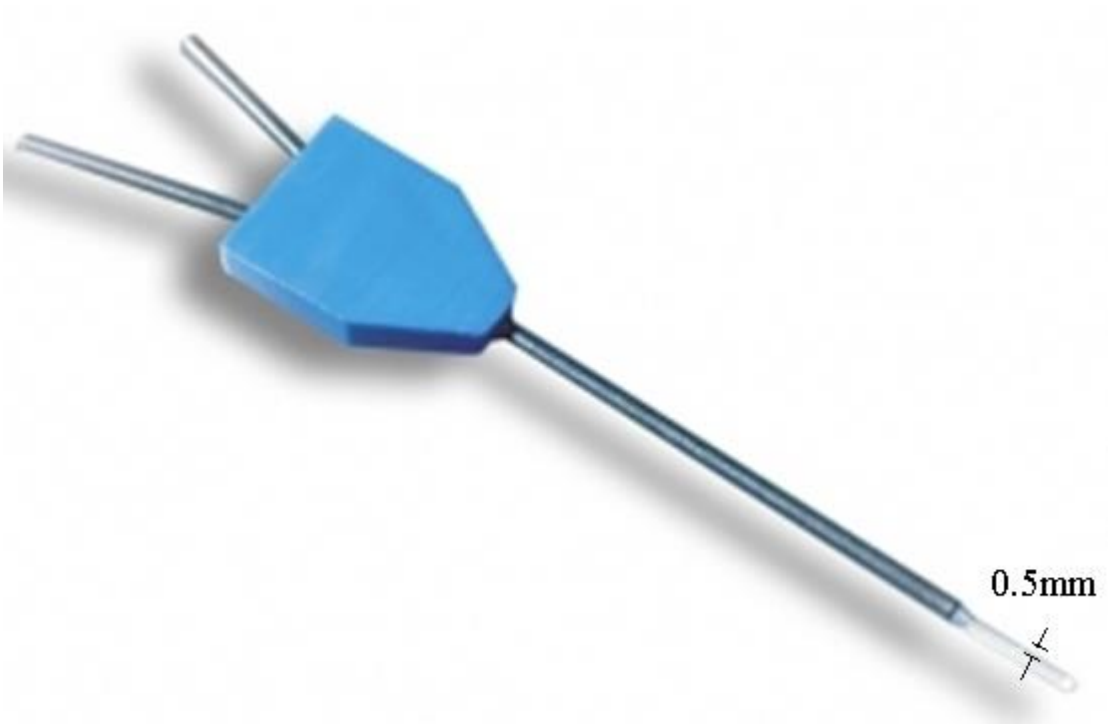

Figure 2 is a picture of a CMA 12 microdialysis probe. This picture was taken from the CMA product catalog, and the dimension was added **[6]**.

The following three figures, Figure 3, Figure 4, and Figure 5, are three dimensional models created with Auto Desk Inventor. The purpose of these three figures is to clearly illustrate the geometry of the microdialysis probe. The easiest way to understand the geometry of a microdialysis probe is to think about them as a cylinder within a cylinder.

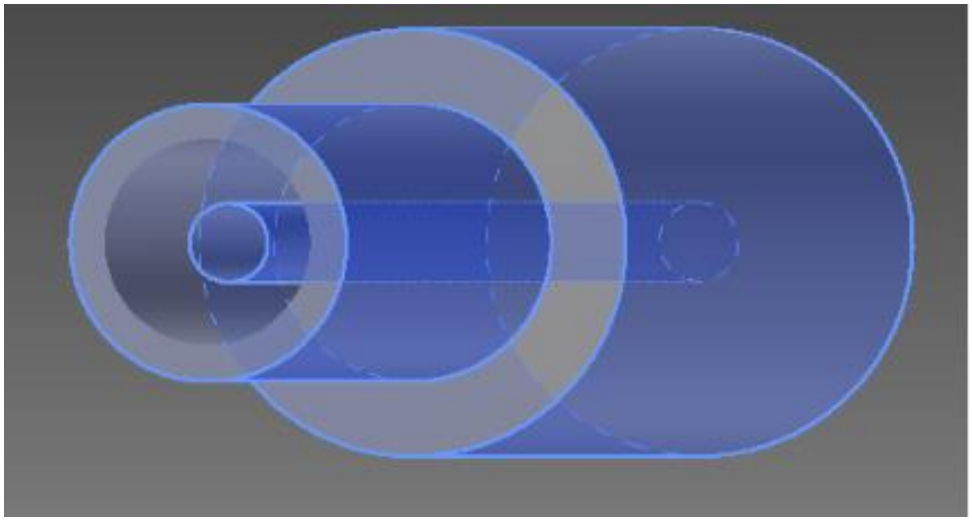

Figure 3 is a three dimensional scale model of a microdialysis sampling probe.

Figure 4 has been altered to highlight the inner cylinder, known as the cannula. The cannula is where the flow enters the probe.

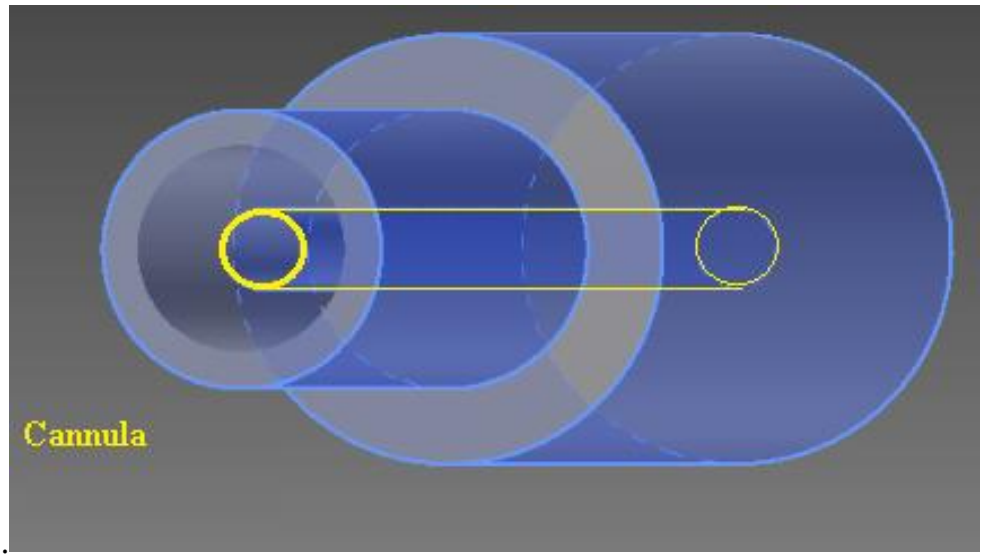

Figure 4 is a three dimensional scale model of microdialysis sampling probe that highlights the cannula in yellow.

Figure 5 has been altered to highlight the outer cylinder in red. The outer cylinder is made up of the membrane and the polyurethane shaft. The volume between the outer cylinder and the inner cylinder is known as the annulus.

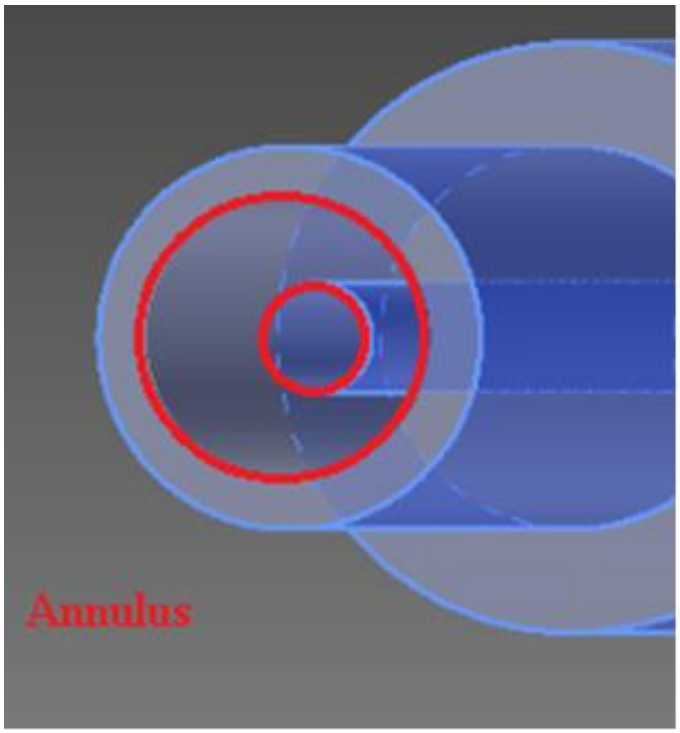

Figure 5 is a three dimensional scale model of microdialysis sampling probe highlighting the annulus in red.

Table 1 is a list of radial distances for the CMA 20 and CMA 12 microdialysis probe that were found in literature [7]. These values were used to calculate the results in this work and will be referred to later.

Parameter Definition	Variable	CMA20	CMA12	Units
Membrane Length	L_m	10.0	4	mm
Radial Distance from the central axis to the outer surface of the cannula	r_{oc}	175	125	μm
Radial distance from the central axis to the inner surface of the semipermeable membrane	r_{im}	210	200	μm
Radial distance from the central axis to the outer surface of the semipermeable membrane2	r_{om}	250	250	μm

Table 1 shows various radial distances of the CMA 20 microdialysis probe given in literature [7].

The physical mechanism by which the microdialysis sampling probe collects is diffusion. Figure 6 shows an overview of how a microdialysis probe works. Before the fluid enters into the probe it is known as the perfusate. Once the fluid has made it through the probe it is referred to as the dialysate [3].

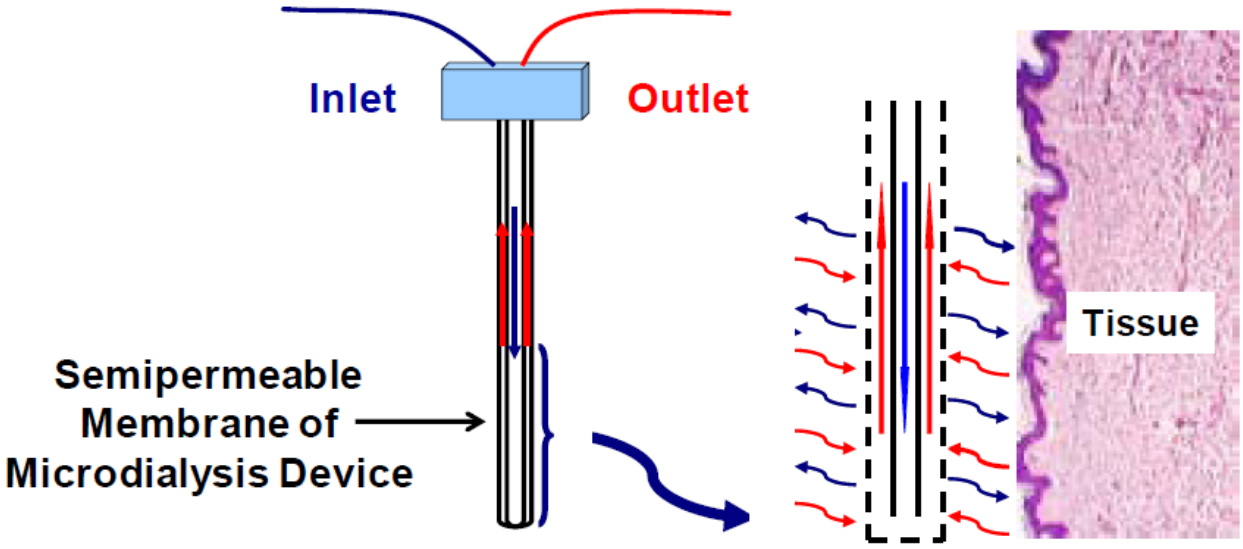

Figure 6 is a depiction of how microdialysis sampling physically occurs. This diagram was acquired from personal communication with Dr. Julie Stenken.

In a typical microdialysis collection a syringe pumps pushes fluid through the inlet tubing into the center cannula. The fluid travels down the cannula to the bottom of the probe. Then, the fluid enters the annulus and flows upward where it can exit the probe via the outlet tubing. While the fluid is in annulus region it interacts with the ECF via diffusion across the semipermeable membrane. This means that direct measurements of the ECF are not made. The inability to make direct measurements of the ECF using microdialysis sampling creates a problem.

1.3 Problem Statement

The problem is that the analyte concentration in the microdialysis sample is rarely equal to the analyte concentration in the medium that was sampled. This means that the precision, and consequently the usefulness, of microdialysis sampling as a method is limited. The extraction fraction is an efficiency metric that quantifies this problem [8]. The extraction fraction, E_d, is the ratio of the perfusate and dialysate analyte concentration difference to the analyte concentration difference between ECF and the perfusate. Equation 1expresses E_d symbolically.

$$\text{Extraction Fraction} = E_d = \frac{C_{Out} - C_{In}}{C_{\infty} - C_{In}} \qquad \text{Equation 1}$$

Equation 1 is used to quantify how efficient a given sampling procedure or microdialysis probe is. E_d can be calculated from its definition with three values, C_{Out}, C_{In}, and C_{∞}, which are the concentration leaving the probe, concentration entering the probe, and the concentration of the surrounding medium, respectively.

The infinity subscript serves as a reminder that the extraction of analytes from the external medium causes a concentration gradient radially very near the probe. This is significant because the assumption is made that the concentration gradient is negligible and consequently the concentration witnessed by the probe is equal to the concentration "very far from the probe" [9].

1.4 Current Solutions

There are currently two prevailing possibilities for dealing with the problem of low percent recovery. The first is to increase the extraction fraction by decreasing the volumetric flow rate. The second approach is to use things that are known, along with mathematical

inference, to quantify, or at least qualify the concentration of analyte within the surrounding medium.

1.4.1 Correlation

To understand E_d and the challenges involved in its calculation consider two cases, in vivo and in vitro microdialysis sampling. The phrase in vivo microdialysis sampling refers to performing microdialysis sampling collections on living organisms. The phrase in vitro microdialysis refers to performing microdialysis collections in a stock solution (usually either in a beaker or test tube) [3].

Consider first in vivo microdialysis sampling. Look at Equation 1. Now, take the time to convince yourself that, in vivo, E_d cannot be calculated directly from its definition. The reason is that, in vivo, C_∞ is not known. Recall, that the value of C_∞ (and how it changes over time) is what we seek to obtain.

Now, consider the second case, in vitro microdialysis sampling. Look at Equation 1. During in vitro microdialysis C_∞ is known. In vitro, C_∞ is the concentration of a stock solution prepared by the researcher, a value that is predetermined by the scientist. [10] .

1.4.2 Upper Limit

A common microdialysis correlation method is to compare in vivo concentrations to known in vitro results. The premise for this idea is that in vivo resistances to diffusion are greater than in vitro resistances. The in vitro data are used to place an upper bound on the expected in vivo recovery. It is common for in vitro data to be used to interpret in vivo data in this way [11] [12].

1.4.3 No Net Flux (NNF)

No net flux (NNF) is a correlation method that allows for quantitative analysis of C_∞. The argument for No Net Flux goes like this: In addition to extraction, microdialysis probes are capable of infusion. If the perfusate concentration is greater than the concentration of the ECF, then diffusion will take place from the probe to the ECF. Flux in this direction causes the dialysate concentration to be lower than the perfusate concentration. These facts lead paired with the original description of microdialysis as a collection method leads to the following algorithm:

If C_{Out} is lower than C_{In}, then C_∞ is lower than C_{In}. If C_{Out} is higher than C_{In}, then the C_∞ is higher than C_{In}. If C_{Out} is equal to C_{In}, then C_∞ is equal to C_{In}. C_{In} is subtracted from C_{Out} and the result is plotted as a function of C_{In}.

An iterative process is carried out to discover C_{In}, such that C_{Out} minus C_{In} is equal to zero. This is referred to as the point of No Net Flux. The idea of No Net Flux is superior to the idea of placing an upper limit on in vivo results with in vivo results, because it allows the researcher to make quantitative remarks, as opposed to qualitative remarks.

There are many examples of No Net Flux being used in biological investigations, such as quantifying extracellular dopamine in the nucleus accumbens during rat amphetamine withdrawal [13], dopamine levels in rat stratium [14], and the pharmacological influences on the in vivo E_d [15]. No Net Flux has also been used to quantify extracellular dopamine in the nucleus accumbens during rat cocaine withdrawal [16], intercellular water space in humans [17], and the coupled effects of mass transfer and uptake kinetics on in vivo microdialysis of dopamine [18].

1.4.4 Slowing Volumetric Flow Rate

Decreasing volumetric flow rate, Q, has been proven, analytically and empirically, to increase E_d. Decreasing Q is the standard operating procedure for bringing the microdialysis sampling concentrations closer to the concentration of the ECF. Bungay et al was the first to use mathematical modeling to describe E_d as a function of known system parameters, such as, the effective system permeability, membrane surface area, and volumetric flow rate, P, S, and Q respectively. Their result is shown in Equation 2.

$$E_d = 1 - e^{\frac{SP}{-Q}} \qquad \text{Equation 2}$$

E_d may also be written in terms of the total system resistance, R, as shown in Equation 3 [9]. P will be treated in more detail in Chapter 3.

$$E_d = 1 - e^{\frac{-S}{QR}} \qquad \text{Equation 3}$$

1.5 New Solution

1.5.1 Introduction to Recycled Flow

Although the idea of decreasing flow rate has had success increasing E_d, this idea has reached a physical limit with the advent of ultraslow flow rates. The term "ultraslow" has been functionally defined as less than 200nL/min. This physical "speed limit" stems from the fact that the flow is so slow that the concentration of the sample will change appreciably due to evaporation before it can be analyzed [19].

1.5.2 Hypothesis

The governing principal behind the hypothesis in this work is that while it is true that decreasing the flow rate increases E_d, it is more general to say that increasing the residency time, T_r, increases E_d. It is trivial to prove which is more general.

First a definition for what it means to be more general must be settled on. It cannot be argued that S_1 is less general than another solution, S_2, if S_1 is a subset of S_2 and S_2 is not a subset S_1. If we let decreasing Q be S_1 and increasing T_Q be S_2, it is clear that S_1 is a subset of S_2. All that remains is to remember that the set S_2 may not be a subset of S_1; unless S_1 is equal to S_2. Since S_1 does not equal S_2, S_2 cannot be a subset of S_1. Therefore, S_1 is a subset of S_2 and S_2 is not a subset S_1. Consequently S_2 is more general than S_1.

The residency time, T_R as described by Bungay et al is shown in Equation 4. L, r_{im}, and r_{oc} are the, membrane length, radial distance to the inner surface of membrane, and the radial distance to the outer surface of the cannula, respectively. Equation 4 is derived by subtracting the volume of the inside cylinder from the volume of the outside cylinder, and dividing by the Q (neglecting the transition at the end).

$$T_R = \frac{L\pi}{Q}\left(r_{im}^2 - r_{oc}^2\right) \qquad \text{Equation 4}$$

The hypothesis of this work is that E_d may be increased even while holding the Q constant by recycling the dialysate flow back through the microdialysis probe. Furthermore, E_d can be written as a function of the number of times a given volume of dialysate passes through the probe, $\#_P$. Finally, as an extension of the main hypothesis it was hypothesized that E_d may be increased at a constant Q even as MW increases.

1.6 Extrapolation to Higher MW Molecules

1.6.1 Motivation for extrapolation to higher MW molecules.

According to expert researchers in the field more than 90 percent of the papers that have been published on microdialysis have been focused on neuroscience [3]. The need to research neurotransmitters cannot be overstated; however neurotransmitters are not the only class of signaling molecule that are important.

Signaling proteins are an example of an important class of signaling molecule that needs further investigation. As researchers continue to learn more about how to use the presence of biomarkers (or their absence) as an indication of disease states biomarker observation will become increasingly important. Another general example is the neuropeptides that govern our human bodies' immune and foreign body response [8].

The reason so much attention has been paid to neurotransmitters relative to other signaling proteins is likely because neurotransmitter are collected with more success relative to other signaling molecules. The diffusivity of a molecule is dependent on the MW of that molecule. E_d is higher when collecting neurotransmitters as compared to E_d when collecting proteins, because neurotransmitters have a higher rate of diffusion relative to proteins. To put things into perspective consider that even if the molecular cutoff weight of the membrane is 100 kDa and the protein is 10 kDa, recovery is still likely to be below five percent [11].

1.6.2 Defining the Diffusive Flux

Equation 5 is the definition of the diffusive flux, J. J is the amount of material crossing a surface at a given time. D is the free aqueous diffusion coefficient. J has a linear relationship with the concentration change,$\nabla\emptyset$ [20]. Equation 5 says that as the concentration gradient across a surface increases so does the flux across that surface.

$$J = -D\nabla\emptyset \qquad \text{Equation 5}$$

1.6.3 A Closer Look at Effect of MW on the Diffusion Coefficient

For a closer look at the effect that MW has on the diffusion coefficient, the best place to start is with the Stokes-Einstein relation shown in Equation 6. By making a few simplifying assumptions an estimate of the relationship between the diffusion coefficent of a particle and its MW can be derived. Consider an uncharged particle, having radius, r, in a medium of constant viscosity, η, and temperature, T. D is the free aqueous diffusion coefficient. [21] [22]. k_B is the Boltzmann constant.

$$D = \frac{k_B T}{6\pi\eta r} \qquad \text{Equation 6}$$

In order to see the relationship between D and the size of the particle more clearly a constant K_1 is defined in Equation 7.

$$K_1 = \frac{k_B T}{6\pi\,\eta} \qquad \text{Equation 7}$$

Substituting K_1 into Equation 6 results in Equation 8, from which it is clear that D is inversely proportional to r.

$$D = \frac{K_1}{r} \qquad \text{Equation 8}$$

1.6.3.1 Justification for Assuming K_1 is constant

The constant K_1 in Equation 7 is potentially a function of many things including temperature and viscosity of the medium. It is worthwhile to consider these things and realize what variable will be rate limiting within living tissue. Look at Equation 7 and take the time to convince yourself that the rate limiting variable will be the variable with the largest range.

For a molecule in the ECF under normal conditions, changes in temperature will be on the order of a few degrees. The viscosity of the ECF will have an appreciable effect on localized diffusion and consequently will have an effect on cell communication [23]. However, analogous to temperature most living organisms have internal processes that monitor and regulate changes in viscosity [24]. The ECF viscosity will always be of the same order of magnitude. In fact it will be approximately equal to the viscosity of water [25]. The MW of a neurotransmitter and protein may vary by as much as three orders of magnitude [8]

It is clear that the variable with the greatest variance is the MW. Therefore, it can be concluded that the variance of the aqueous diffusion coefficient for various molecules in the ECF is due to the differing MW of the various molecules.

1.6.3.2 Writing D in Terms of its Mass and Density

Assuming a spherical shape the relationship between a molecules's MW, M_w, and its radius, r, is shown in Equation 9. ρ is the density of the particle and N is Avogadro's number.

$$M_w = N\rho\frac{4}{3}\pi r^3 \qquad \text{Equation 9}$$

Solving Equation 9 for r, substituting the result into Equation 8, and defining a new constant K_2 as in Equation 10, results in Equation 11.

$$K_2 = \left(\frac{3}{4\pi N}\right)^{\frac{1}{3}} \qquad \text{Equation 10}$$

$$D = \frac{K_1}{K_2} * \left(\frac{\rho}{M_w}\right)^{\frac{1}{3}} \qquad \text{Equation 11}$$

It is true that most molecules are not spherical, in fact, most are far from it. However, this exercise is useful because it illustrates the relationship between the free aqueous diffusion coefficient of a particle and that particle's MW.

Chapter 2: Experimental Methods

2.1 Chemicals:

High Pressure Liquid Chromatography (HPLC) Water, Fluorescein isothiocyanate dextran 4 (FITC-4), dimethylaminoazobenzene-4'-sulfonic acid (methyl orange) were purchased from Sigma Aldrich (California USA).

2.2 Equipment and Materials

A CMA Liquid Switch, CMA 402 Syringe Pump, FEP tubing and associated connectors were purchased from CMA Microdialysis, North Chelmsford, MA. A VWR Mini Pump Variable Flow was purchased from VWR International.

2.3 Methods

2.3.1 Work Flow

Figure 7 illustrates the work flow for the experimental process.

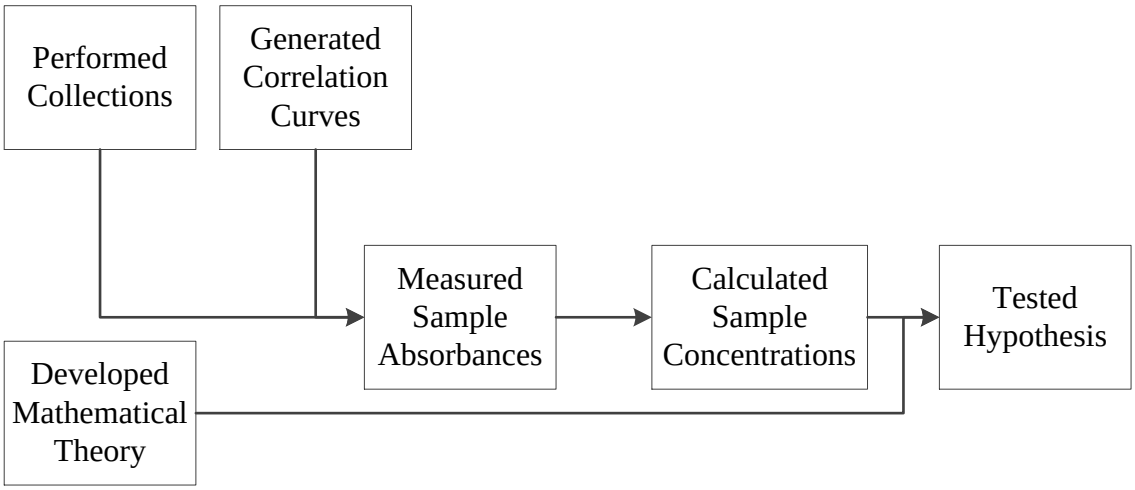

Figure 7 is a process diagram that describes the flow of work during the experimental process.

First an absorbance correlation curve was created solutions of known concentration. In vitro collections were performed and absorbance of the collection was measured. These intensities were translated to concentrations via the correlation curves that were created. Then resulting concentrations were translated into E_d using Equation 1. The resulting E_d was plotted versus $\#_p$. These plots were used to demonstrate that E_d increases as the $\#_p$ increases.

2.3.2 Method Recycled Flow

2.3.1.1 Design Goals

There were three initial design goals. The first goal was to direct the flow leaving the probe back into the inlet of the probe so that a second pass through the probe could be accomplished. The second goal was that the system be able to complete multiple passes in addition to the second pass and to have the capacity to continue cycling for long periods of time. The third goal was that it be possible to determine how many cycles each sample had made and equivalently that it be possible to sample at arbitrary specified cycle numbers.

2.3.1.2: Recycled Flow System State Diagrams

Functionally there are three possible states that the recycled flow system may exist in, State 1, State 2, and State 3. State 1 was used for priming the lines, collecting data on the first pass, and returning the system to a state where the perfusate in the system (past the probe) has experienced one pass. State 2 was used for cycling. State 3 is collection.

Figure 8 illustrates State 1 and State 3. While in State 1 the perfusion fluid was pulled from a fluid reservoir, through the liquid switch and the microdialysis probe, to the peristaltic pump. In Figure 8 this is path ABC. Once through the peristaltic pump the fluid was pushed

into the liquid switch, D. Lastly the dialysate solution traveled to the Collection, E. The distinction between State 1 and State 3 is that State 1 takes place before cycling and State 3 takes place after cycling.

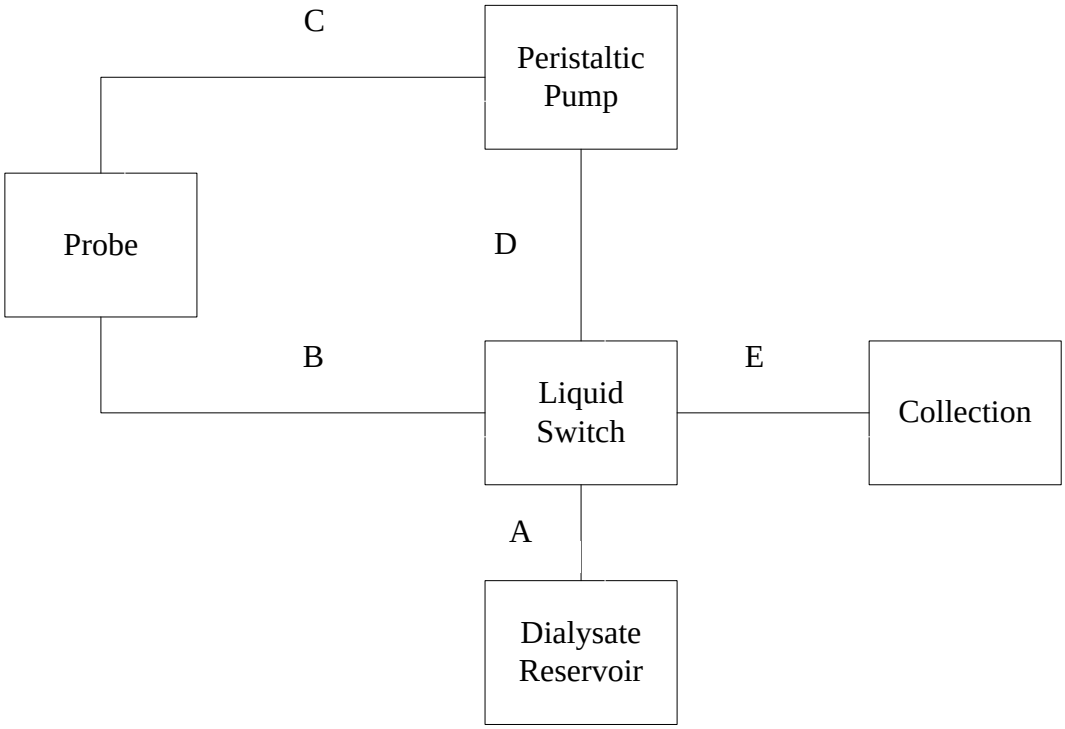

Figure 8: Recycled Flow State 1 and State 2 Operational Flow Chart

State 2 is illustrated in Figure 9. While in State 2 the flow is recycled through the probe, peristaltic pump, and liquid switch, path CDB.

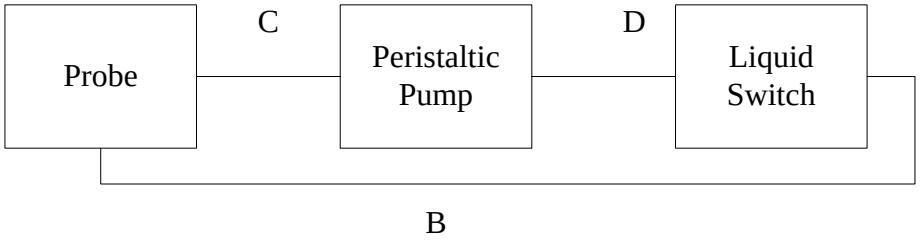

Figure 9: Recycled Flow State 2 Operational Flow Chart

2.3.1.3 Recycled Flow Description of Experiments

Recycled flow microdialysis experiments were performed in the following way. After stirring the stock solution for 15 minutes to ensure homogeneity of the solution, a 50 mL beaker was filled with a 100µM stock solution and a magnetic stirring rod was placed in the solution. The beaker was covered with parafilm to limit evaporation. A small cross was cut in the center of the parafilm with a razorblade through which a microdialysis probe was inserted. Two small alligator clips were clamped on opposite sides at the base of the probe to ensure that the microdialysis probe remained upright.

Methyl orange and p-nitroaniline were cycled with the VWR variable speed pump at 5µL/min. FITC-4 Dextran was cycled with the Harvard Apparatus peristaltic pump at 1µL/min. The peristaltic pump was activated and the dialysate was allowed to fill the system and flow into a 50 mL waste beaker for 30 minutes to ensure the system reached equilibrium. At this point one pass samples were taken. The system was then placed into State 2 and so that the perfusate could be subjected to multiple passes through the probe. After cycling was completed the system was placed into State 3, so that the sample could be removed from the system.

Three different analytes were collected, methyl orange, p-nitroaniline and fluorescence isothiocyanate dextran-4 (FITC-4). Methyl orange was collected with both types of CMA 20

microdialysis probe (PAES and PES). A CMA 20 PES microdialysis probe was used to collect p-nitroaniline. A CMA 12 PES was used to collect FITC-4. Table 2, Table 3, Table 4, and Table 5 show what numbers of passes were used and the number of times each pass number was carried out, for methyl orange PES, methyl orange PAES, p-nitroaniline, and FITC-4 Dextran, respectively.

$\#_p$	1	3	5	7	9	11	13	15	24
n	4	3	4	3	3	3	2	1	1

Table 2 shows, for methyl orange (PES), the various #p that were investigated and the number of times the investigation was duplicated.

$\#_p$	1	3	5	7	9	11	13	22
n	9	3	7	3	5	4	1	1

Table 3 shows for, methyl orange, the various #p that were investigated and the number of times the investigation was duplicated.

$\#_p$	1	2	4	6	8	15
n	4	4	4	4	4	8

Table 4 shows, for p-nitroaniline, the various #p that were investigated and the number of times the investigation was duplicated.

$\#_p$	1	3	5	7	9	11
N	3	3	3	3	3	3

Table 5 shows, for FITC-4, the various #p that were investigated and the number of times the investigation was duplicated.

2.4 Traditional Microdialysis

2.4.1 Traditional Microdialysis State Diagram

Figure 10 is a state diagram for traditional microdialysis. Fluid is pushed through the microdialysis sampling probe by a syringe pump. When the fluid leaves the probe it is pushed off to collection. It is worth noting here that traditional microdialysis has only one state.

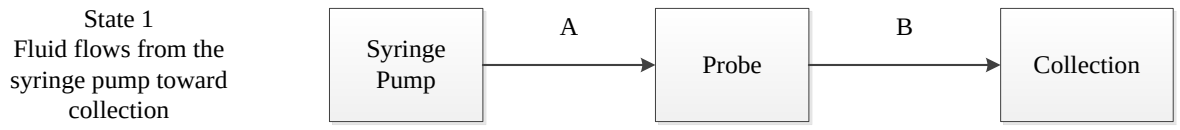

Figure 10 is a state diagram for traditional microdialysis

2.4.2 Traditional Microdialysis Description of Experiments

Traditional microdialysis was performed in the following way. After stirring the stock solution for 15 minutes to ensure they were homogeneous, a 50 mL beaker was filled with a 100µM stock solution. A magnetic stirring rod was placed in the solution. The beaker was covered with parafilm to limit evaporation. A small cross was cut in the center of the parafilm with a razorblade through which a microdialysis probe was inserted. Two small alligator clips were clamped on opposite sides at the base of the probe to ensure that the microdialysis probe remained upright.

A CMA 402 syringe pump was attached to a CMA 20 PAES microdialysis probe in the methyl orange solution. The syringe pump was activated and the dialysate was allowed to fill

the system and flow into a 50 mL waste beaker for 30 minutes to ensure the system reached equilibrium. Collections were performed at several flow rates (1, 2, 4, 5, 8, and 10μL/min). The collection volume, 100μL, was held constant each time. Table 6 shows the number or measurements, n, taken at each flow rate.

$Q\left(\frac{\mu L}{min}\right)$	1	2	4	5	8	10
N	2	2	5	3	3	3

Table 6 shows the flow rates that were investigated and the number of times they were duplicated.

2.4 Analysis

2.4.1 Instrumentation

Absorbance measurements were accomplished using the Thermo Scientific Nano Drop 2000c, (Wilmington, DE).

2.4.2 Determining sample concentration from emission intensity

Five separate 50 μL standards of known molar concentrations were prepared. Absorbance intensity measurements were made and the values were recorded. This was carried out three times so that there were three sets of absorbance intensity versus analyte concentration data. The mean of the three intensities was used to generate a scatter plot of intensity versus concentration. This scatter plot was fit with a regression line. The regression line equation and the collection samples measured intensity was then used to calculate the unknown concentrations of the samples collected during the procedure.

Chapter 3: Theory

3.1 Derivation of Theoretical E_d as a Function $\#_P$

Chapter 3 describes the efforts made to theoretically predict the necessary number of passes to achieve complete recovery. The result of this effort is an equation for the number of passes as a function of the extraction fraction.

Imagine an object of velocity v. If we know the time, t, that the object maintains that velocity, we can calculate the distance traveled d. This general case is represented in Equation 12.

$$d = v * t \qquad \text{Equation 12}$$

Imagine now the object is traveling around a loop whose length is L_L and that we restrict the object to completing only an integer number of passes at a constant v. We can now write the distance traveled, L_{Total} as shown in Equation 13.

$$L_{Total} = \#_p * L_L \qquad \text{Equation 13}$$

From this we can see that the number of cycles that a given volume completes is equal to the total distance traveled divided by the length of the loop, as shown in Equation 14.

$$\#_p = \frac{L_{Total}}{L_L} \qquad \text{Equation 14}$$

Now imagine our object is a volume of fluid moving through a tube. We may choose to define Q_1 as the Q necessary for a given volume of fluid to make one cycle given that the crossectional area of the tubing is A_C, the length of the loop is L_L, and the time to complete one revolution is T_L. P is the overall system permeability. The relationship between these quantities is shown in Equation 15.

$$Q_1 = \frac{A_C * L_L}{T_L} = \frac{\#_P * T_L * P}{A_C * L_{Total}} \quad \text{Equation 15}$$

Substituting Q_1 into Equation 2 leads to Equation 16.

$$E_d = 1 - \exp\left(\frac{-T_L * P * A_S}{A_C * L_L}\right) \quad \text{Equation 16}$$

Combining Equation 13 and Equation 16, we may write the E_d in terms of the number of passes. This relationship is shown below in Equation 17.

$$E_d = 1 - \exp\left(\frac{-\#_P * T_L * P * A_S}{A_C * L_{Total}}\right) \quad \text{Equation 17}$$

A_S is calculated using L and r_{om} from Table 1 and the formula for the surface area of a cylinder. A_C is calculated from the diameter of the tubing, which is provided by the tubing manufacturer. P will require further exploration.

There are three permeabilities to consider with respect to microdialysis sampling. These are the permeabilities of the dialysate within the probe annulus, probe membrane, and the external medium, P_d, P_m and P_∞, respectively. Equation 18 shows the relationship between the effective system permeability and the actual individual permeabilities [9].

$$P = \left(\frac{1}{P_d} + \frac{1}{P_m} + \frac{1}{P_\infty}\right)^{-1} \quad \text{Equation 18}$$

Bungay et al have derived expressions for P_m and P_d in terms of geometric probe dimensions, the radial distance to the outside surface of the inner cannula, the radial distance to the inner surface of the membrane, and the radial distance to the outer surface of the membrane, r_{oc} , r_{im}, and r_{om}, respectively [9]. Earlier work from Bungay describes the analogous resistances [26]. These expressions for P_d and P_m are given in Equation 19 and Equation 20. D_m is the

diffusion coefficient of the analyte through the membrane. D_d is the diffusion coefficient of the dialysate fluid.

$$P_d = \frac{35}{13} * \frac{D_d}{(r_{im} - r_{oc})} \quad \text{Equation 19}$$

$$P_m = D_m * \left(r_{im} * \ln(\frac{r_{om}}{r_{im}}) \right)^{-1} \quad \text{Equation 20}$$

In general, the permeability varies with axial position. This variance is considered to be negligible as long as r_{im}-$r_{oc} \ll r_{oc.}$ This approximation has been confirmed by Wallgren et al [27]. As long as the experiment is in vitro and the medium remains well stirred we can neglect P_∞ [9]. Combining Equation 18, Equation 19, Equation 20, and defining two new constants results in Equation 21.

$$P = \left[\frac{K_3}{D_d} + \frac{K_4}{D_m} \right]^{-1} \quad \text{Equation 21}$$

Equation 22 and Equation 23 define the constants K_3 and K_4, respectively.

$$K_3 = \frac{13 * (r_{im} - r_{oc})}{35} \quad \text{Equation 22}$$

$$K_4 = r_{om} * \ln \frac{r_{om}}{r_{im}} \quad \text{Equation 23}$$

Defining another constant, K_5, shown in Equation 24, and combining Equation 17, Equation 18, Equation 21, and Equation 24, results in Equation 25.

$$K_5 = \frac{T_L * A_S}{A_C * L_{Total}} \quad \text{Equation 24}$$

$$E_d = 1 - \exp\left[(-K_5\ \#_P)\left(\frac{K_3}{D_d} + \frac{K_4}{D_M}\right)^{-1}\right] \quad \text{Equation 25}$$

Look at Equation 25. Take the time to convince yourself that for $\#_p$=1, the ratio of the loop time and the total time is equal to the reciprocal of the linear velocity.

D_d for a particular analyte may be calculated using Equation 11. Solving Equation 25 for D_d, results in Equation 26.

$$D_d = -K_3 * [\frac{K_5 * \#_P}{\ln(1 - E_d)} + \frac{K_4}{D_m}]^{-1} \quad \text{Equation 26}$$

Solving Equation 25 for D_m, results in Equation 27. D_m for a particular analyte can be calculated with Equation 27.

$$D_m = -K_4 * [\frac{K_5 * \#_P}{\ln(1 - E_d)} + \frac{K_3}{D_d}]^{-1} \quad \text{Equation 27}$$

Defining a constant K_6 as in Equation 28 we can write Equation 29.

$$K_6 = K_5\left(\frac{K_3}{D_d} + \frac{K_4}{D_m}\right)^{-1} \quad \text{Equation 28}$$

$$E_d = 1 - e^{-K_6 \#_P} \quad \text{Equation 29}$$

3.2 Alternate Method for Calculating Membrane Diffusion Coefficients

If we treat the $\#_p$=1 collections as a traditional microdialysis collection, the diffusivity of the probe can be obtained from Equation 2. The diffusivity of the probe, D_p, is the permeability of the probe multiplied by the thickness of that membrane, T_m.

$$D_p = P\ T_m \quad \text{Equation 30}$$

The thickness of the membrane is calculated by Equation 31.

$$T_m = r_{om} - r_{im}$$ Equation 31

Given a specific membrane, A_s is calculated using Equation 32. Given E_d and Q data, D_p is calculated using Equation 33.

$$A_s = 2\pi * r_{om} L + \pi * r_{om}^2$$ Equation 32

$$D_p = Q \frac{(r_{om} - r_{im})}{A_s} \ln(1 - E_d)$$ Equation 33

Chapter 4: Results, Analysis and Discussion

4.1 Recycled Flow E_d

The extraction efficiencies that where realized while using recycled flow microdialysis sampling to collect from a 100 µM solution of methyl orange are illustrated in Figure 11 and Figure 12. Figure 11 shows the data collected with the CMA PES microdialysis sampling probe. The data are plotted as a function of the number of passes completed. Equation 29 was used to specify the form of the curve fit.

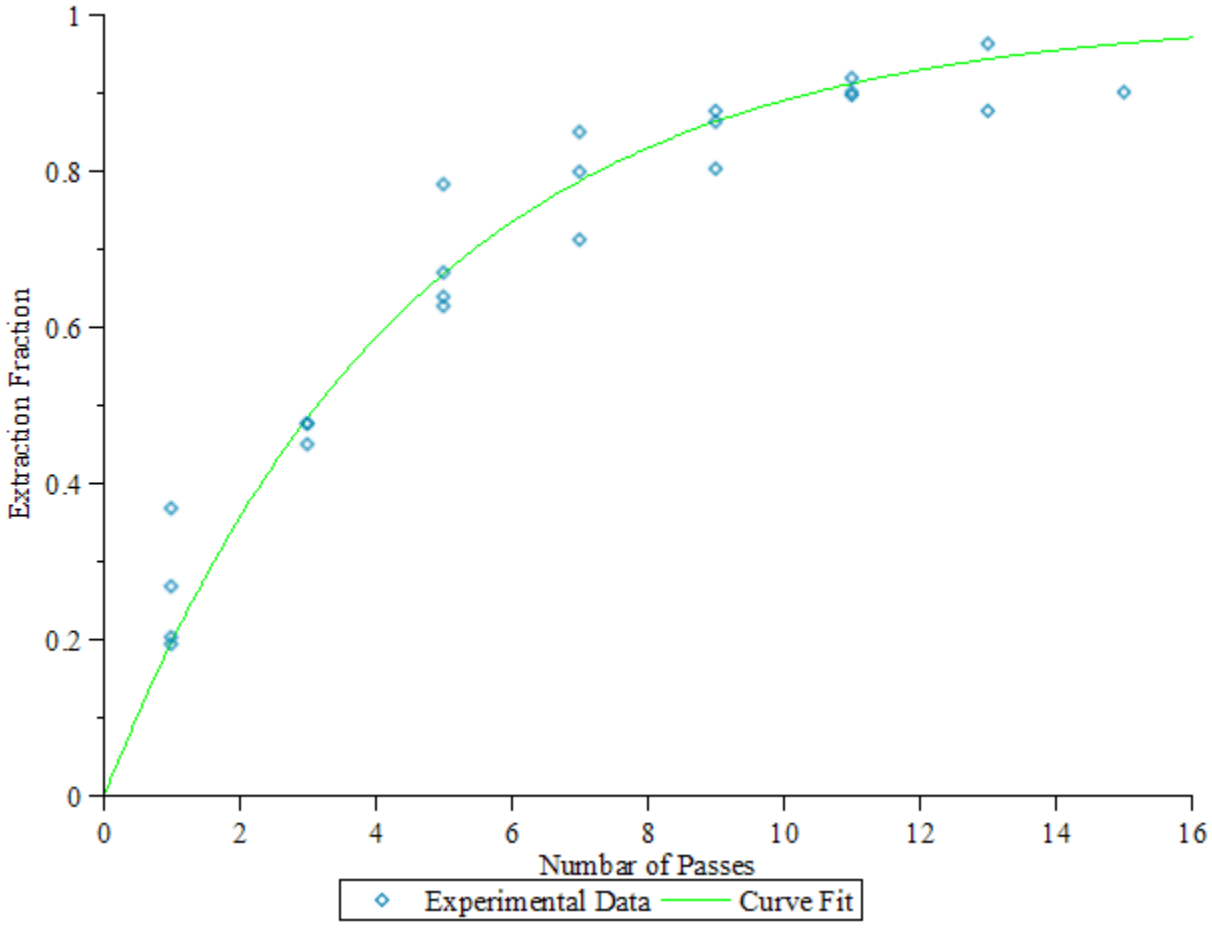

Figure 11: Curve fit superimposed on methyl orange extraction efficiency data collected with CMA 20 PES.

Figure 12 shows the data collected with the CMA PAES microdialysis sampling probe. The data are plotted as a function of the number of passes that was completed. Equation 29 was used to specify the form of the curve fit.

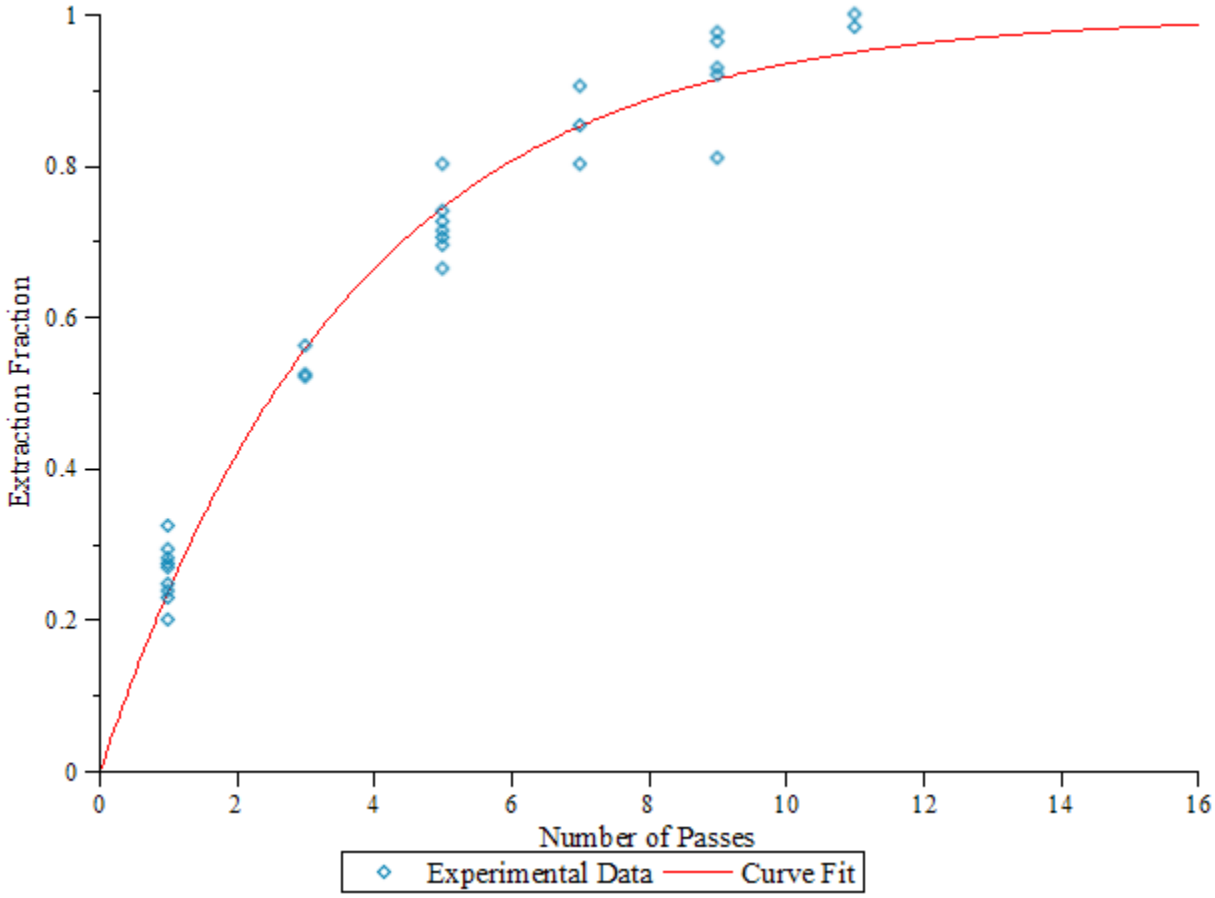

Figure 12: Curve fit superimposed on methyl orange extraction efficiency data collected with CMA 20 PAES.

The extraction efficiencies that where calculated while using recycled flow microdialysis sampling to collect p-nitroaniline is illustrated in Figure 13. The data are plotted as a function of the number of passes that was completed. Equation 29 was used to specify the form of the curve fit.

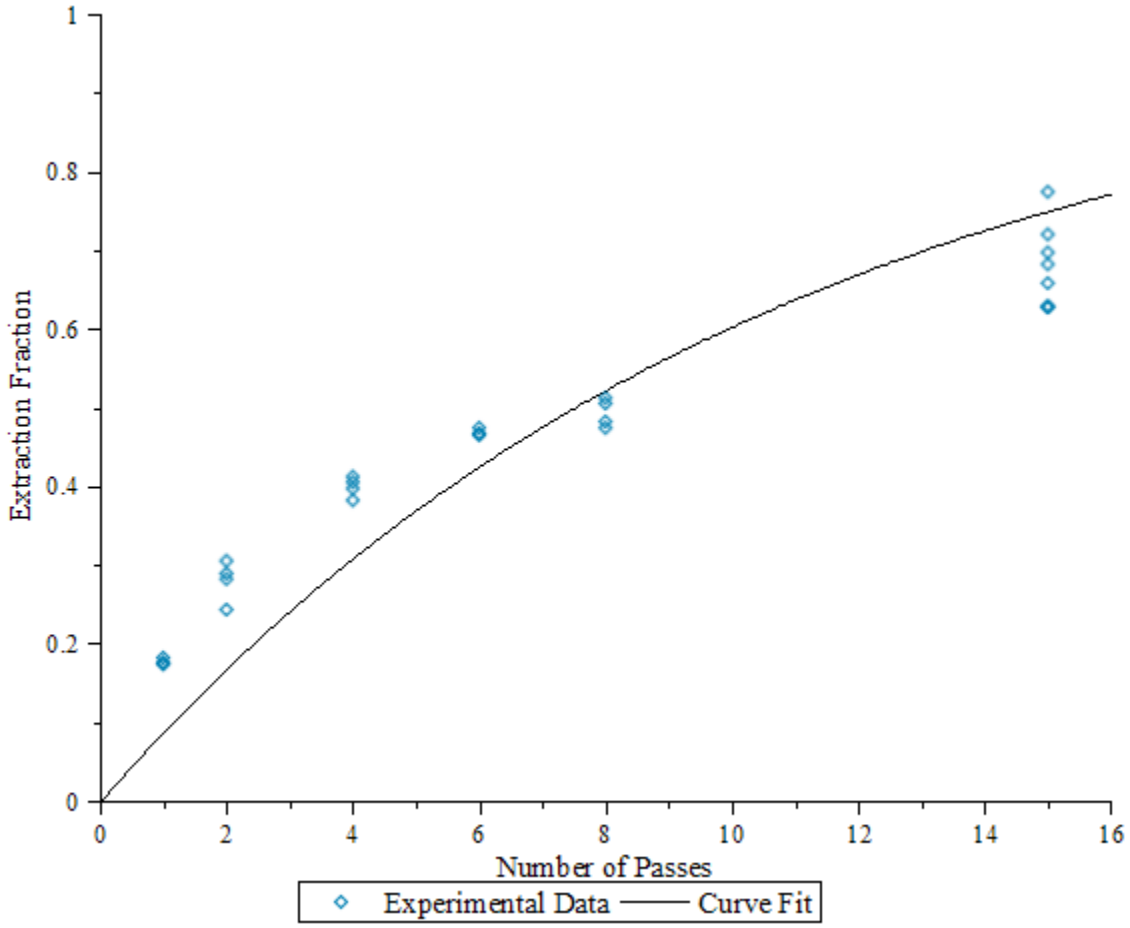

Figure 13: Curve fit superimposed on p-nitroaniline extraction efficiency data collected with CMA 20 PES.

The extraction efficiencies that where calculated while using recycled flow microdialysis sampling to collect FITC-4 Dextran is illustrated in Figure 14. The data are plotted as a function of the number of passes that the sample completed. Equation 29 was used to specify the form of the curve.

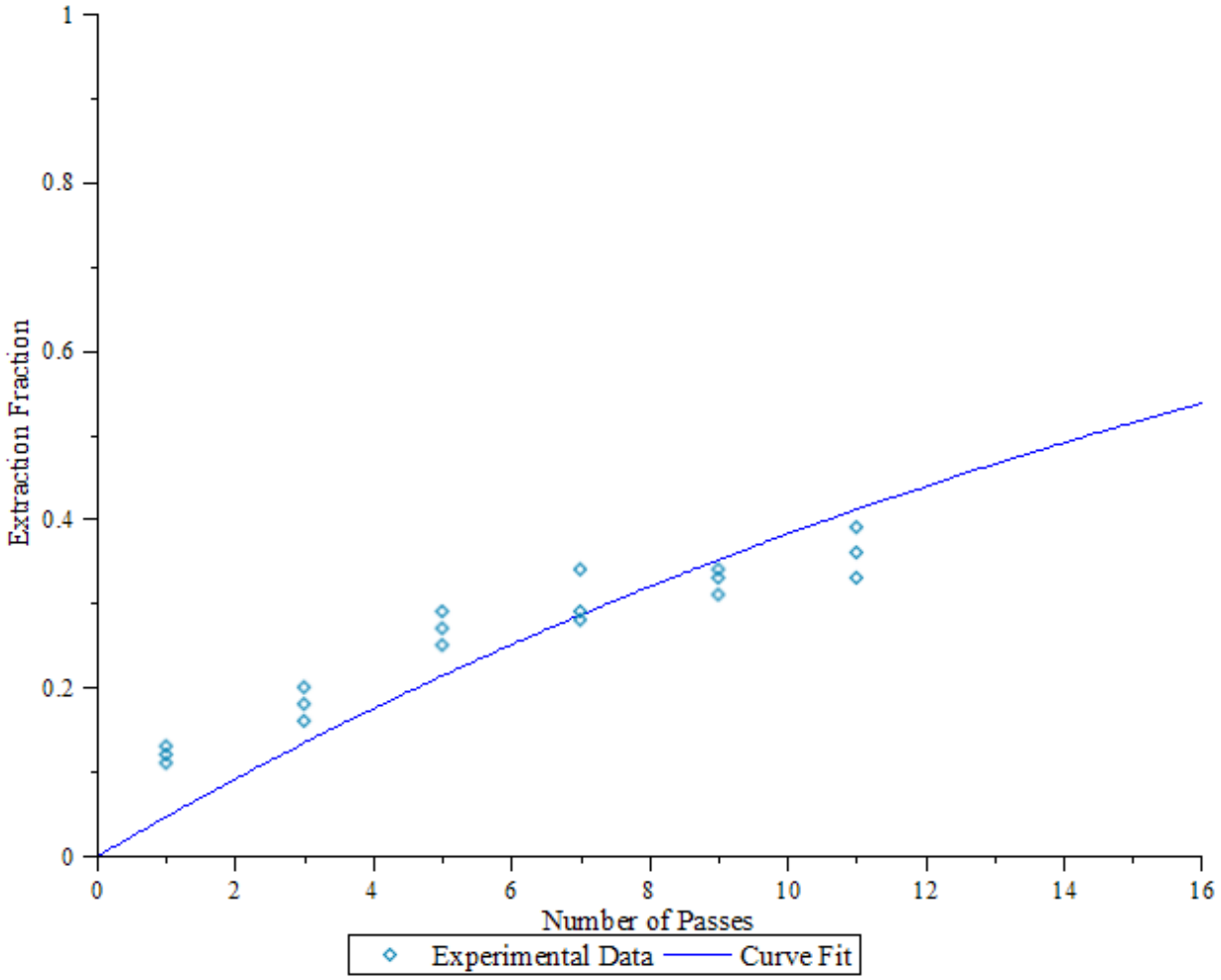

Figure 14: Curve fit superimposed on FITC-4 extraction efficiency data collected with CMA 12 PES

4.2 Curve Fit Equations

4.2.1 Experimentally Determine Values of K_6

The values of K_6 that provided the best fit to the specified form of Equation 29 are given in Table 7.

Analyte	Probe	K_6
FITC-4 Dextran	PES	0.049
methyl orange	PES	0.273
methyl orange	PAES	0.252
p-nitro aniline	PES	0.098

Table 7: Values of a K_6 used for curve fit equations

It is informative to look at all of the curve fit equations plotted simultaneously. Figure 15 illustrates all four of the curve fits. The increase E_d as $\#_p$ increases is evident in all four of the curves. Remembering that all of these molecules have different MW leads to the conclusion that the increase in E_d across various MW is also achievable.

The curves are expected to have an asymptotic behavior as the number of passes goes to infinity. The expected asymptotic behavior is evident in the methyl orange curves but not in the curves fit to the p-nitroaniline and FITC-4 Dextran data.

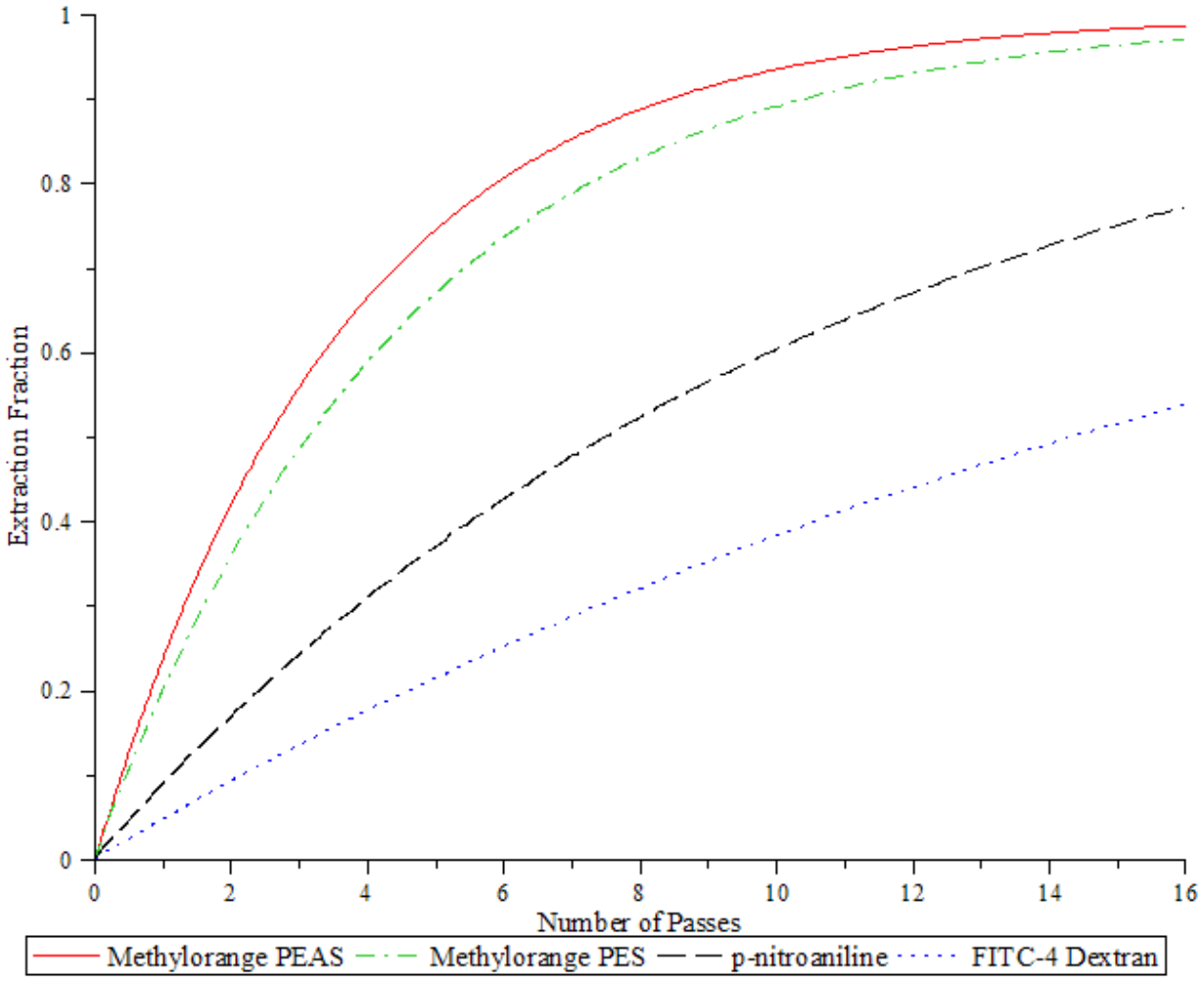

Figure 15 displays all four of the curve fit eqution simultaneously.

Values for K_1 and K_2, MW, and density of each analyte, where used in conjunction with Equation 11 to calculate the free aqueous diffusion coefficients for each analyte used in this study. These results are shown below in Table 8.

	MW	Density	Aqueous Diffusion Coefficient
	kg/mol	kg/m^3	m^2/s
p-Nitroaniline	0.138	1440	6.36E-07
Methyl orange	0.327	1280	4.60E-07
FITC-4 Dextran	4	1383	2.05E-07

Table 8: Diffusion coefficients calculated from Equation 11.

The probe dimensions given in Table 11 and the free aqueous diffusion coefficients shown in Table 8 was used to calculate the values of K_1, K_2, K_3, K_4, and K_5, which are shown below in Table 9.

Defined Constants	CMA20	CMA12	Units
K_1	2.15E-16	2.15E-16	m^3/s
K_2	7.35E-09	7.35E-09	(mol)^(1/3)
K_3	1.30E-05	2.79E-05	M
K_4	4.36E-05	5.58E-05	M
K_5	1.91E+05	3.89E+05	No Units

Table 9 displays the values calculated for K_1, K_2, K_3, K_4, and K_5.

4.2 Validation of Calculated Aqueous Diffusion Coefficient

The validity of these calculated aqueous diffusion coefficients are evident when compared to literature. The data shown in Table 10 are the aqueous diffusion coefficients calculated by Wang et al for Dextran 70, Dextran 40, Dextran 20, and Dextran 10. The Dextran 4 data shown in Table 10 is the value that was shown previously in Table 8. The data from the literature was calculated in a similar manner, using the Stokes-Einstein equation, except they used a Stokes radius provided by the manufacturer instead of deriving it [7].

FITC-Dextran	Calculated D (cm^2/s)
70	5.6x10-7
40	7.4x10-7
20	10.1x10-7
10	14.5x10-7
4	20.5x10-7

Table 10 contains the diffusion coefficients calculated by Wang et al for Dextran 70, Dextran 40, Dextran 20, and Dextran 10 [7].

The data from Table 10 is plotted in Figure 16. The plot is of the inverse cube root of the MW versus aqueous diffusion coefficient. This plot was expected to be linear. This linearity was observed, confirming the validity of the method by which the aqueous diffusion coefficient

for the FITC-4 Dextran was calculated in this work. By induction this implies that the aqueous diffusion coefficients calculated for p-nitroaniline and Methylorange are also valid.

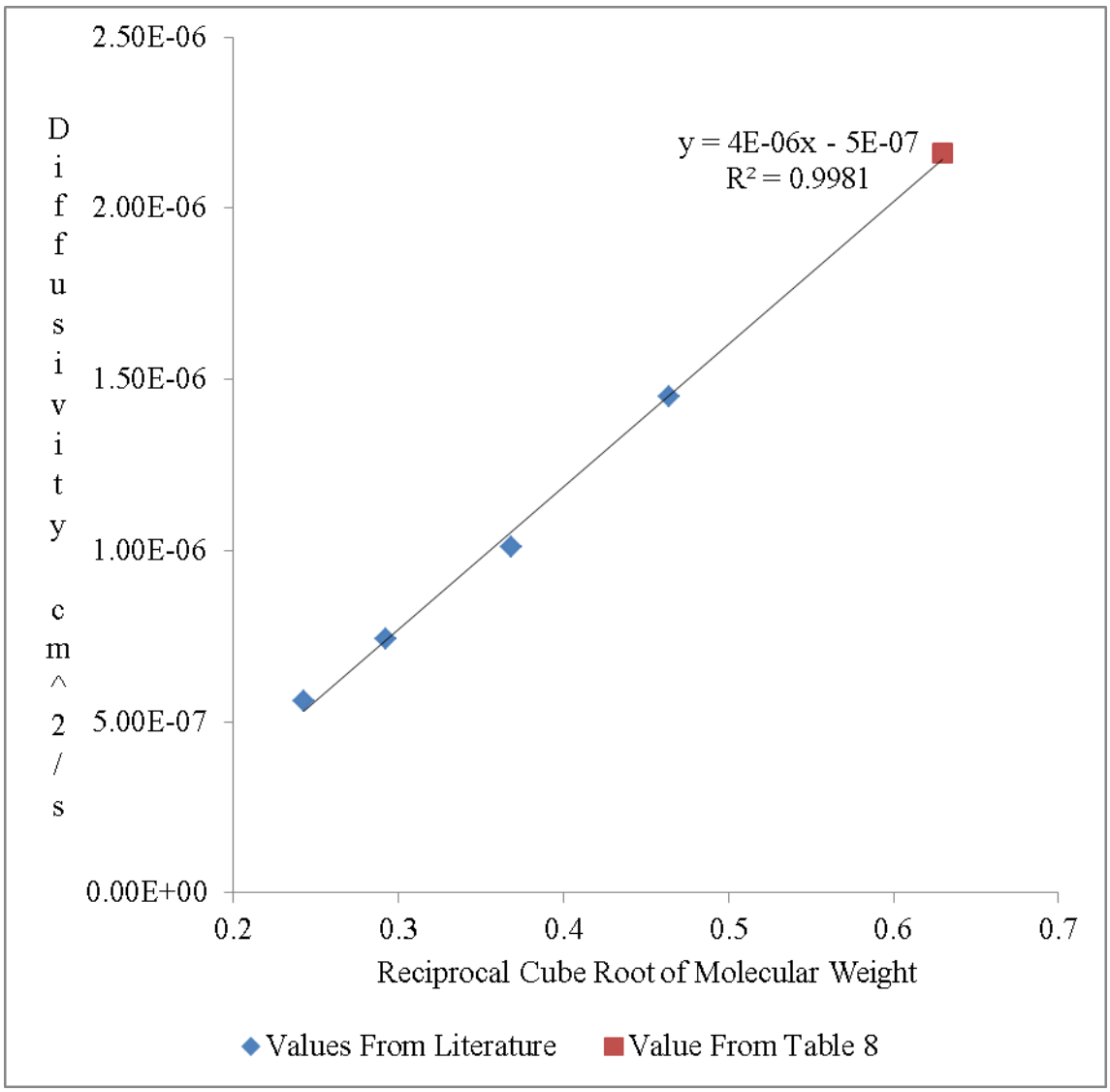

Figure 16 is a plot of the reciprocal of the MW cube root versus the diffusivity for FITC-Dextran 4, 10, 20 40, and 70. The values for FITC-Dextran 10, 20 40, and 70 were taken from literature [7]. The value for FITC-Dextran 4 was taken from Table 8.

4.2 Membrane Diffusion Coefficient Values

Equation 27 was used in conjunction with experimental data to calculate the effective membrane diffusivity for each analyte that was used. These values are shown below in Table 11.

These values were obtained by substituting in 1 for the pass number and the corresponding extraction fraction at that pass.

Analyte	Probe	D_m (m^2)/s
p-Nitroaniline	PES	4.53E-11
Methly orange	PAES	6.78E-11
Methly orange	PES	6.94E-11
FITC-4 Dextran	PES	1.83E-11

Table 11 displays Dm that was calculated using Equation 27.

Equation 33 was used as an alternate way of calculating D_m. These values are reported in Table 12, below.

Analyte	Probe	D_m (m^2)/s
p-Nitroaniline	PES	4.16E-11
Methly orange	PAES	6.23E-11
Methly orange	PES	6.37E-11
FITC-4 Dextran	PES	1.64E-11

Table 12 displays D_m values that were calculated using Equation 33

Analyte	Probe	Percent Change
p-Nitroaniline	PES	9.0
Methly orange	PAES	9.0
Methly orange	PES	9.0
FITC-4 Dextran	PES	11.6

Table 13 displays the percent change in the values that were calculated using Equation 27 and Equation 33.

The most probable explanation for the difference in the values was that the assumption that the permeability would be constant with axial position was not completely valid. r_{ic}-r_{oc}/r_{oc} is equal to 0.2 and 0.6 for the CMA 20 and CMA 12, respectively.

Equation 27 does not consider boundary layer theory. Boundary layers, both velocity and concentration, should have been taken into consideration. Stenken et al measured the effects of boundary layer formation on the outside of a probe and found that a linear velocity lower than

0.211 cm/s affected recovery because of extra resistance due to boundary layer formation. [28]. The linear velocities of the recycled flow experiments were 0.15 and 0.74 cm/s for the CMA 12 and CMA 20, respectively.

4.3 Comparison of Traditional Microdialysis and Recycled Flow Microdialysis

The main purpose of this work was to develop a new method for increasing microdialysis sampling E_d. Since the most widely accepted solution is decreasing volumetric flow rates, it is fitting to compare the two.

The most direct way to compare traditional microdialysis to recycled flow microdialysis is to look at their respective E_d as a function of T_R Figure 17 is a graphical representation of this idea. The recycled flow data are the data from Figure 12. The traditional microdialysis data collection was described in section 2.4.2.

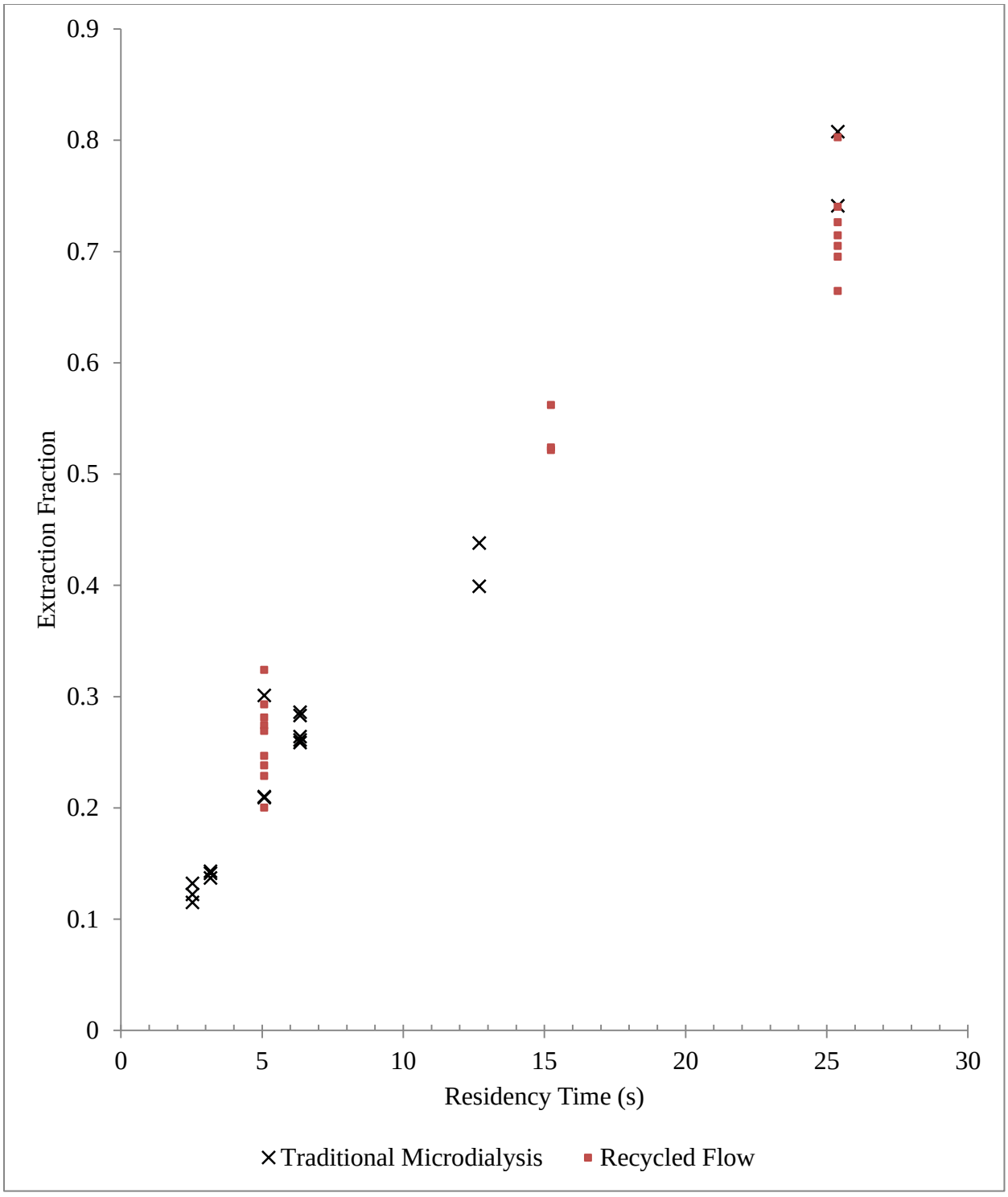

Figure 17 is a graph of traditional and recycled flow microdialysis sampling extraction fraction data plotted as a function of residency time. Black x's represent traditional microdialysis data. Red squares represent recycled flow data.

It was expected that if T_R for traditional/recycled were equal then their respective E_d would also be equal. This expectation was met at 5 and 25 seconds of residency time.

4.4 Discussion and Conclusions

The immediate upside to using recycled flow is that while cycling the samples stay within the lines, not in contact with the atmosphere. This means that the samples are protected from evaporation during cycling. It is also not necessary with recycled flow to use ultraslow flow which means the sample will be protected during collection as well.

In this work the method of recycled flow microdialysis was described and tested. It is concluded that increasing $\#_p$ increases E_d. It is concluded that for the MW tested the increase in E_d can be achieved at different MW. It is also concluded that for the range of T_R tested recycled flow/traditional microdialysis E_d are equal for equal T_R.

In this work a theoretical model was presented to describe E_d at various $\#_p$. The success of the model was varied. It is concluded that the methylorange curve fits seem to have good agreement with the data. It is concluded that the p-nitroaniline and FITC-4 curve fits are not in good agreement with the data. It is clear that future work will be necessary to confirm or deny the disagreement.

Works Cited

[1] L. Berk, K. Krieger and S. Bretscher, Molecular Cell Biology, Freeman, W. H. & Company, 2007.

[2] C. Chaurasia, "In Vivo Microdialysis Sampling: Theory and Application," *Biomedical Chromatagraphy*, pp. 317-322, 1999.

[3] J. Stenken, "Microdialysis: Non-Specialized View," *Encyclepidia of Medical Devices and Instrumentation, Second Edition*, pp. 401-420, 2006.

[4] H. Kalant, "A microdialysis procedure for extracton and isolation of corticosteroids from peripheral blood plasma," *Biochemistry,* pp. 69,99-103, 1958.

[5] U. U and P. C., "Functional Correlates of Dopamine Neurotransmitters," *Bull Schweiz. Akad. Med Wiss.,* pp. 30, 44-45, 1974.

[6] CMA Microdialysis, "CMA Microdialysis Product Catalog," CMA Microdialysis, 5 3 2013. [Online]. Available: http://www.microdialysis.com/us/products/probes. [Accessed 5 3 2013].

[7] J. S. Xiangdan Wang, "Microdialysis Sampling Membrane Performance," *Analytical Chemistry,* vol. 78, pp. 6026-6034, 2006.

[8] X. Ao and J. Stenken, "Microdialysis sampling of cytokines," *Methods 39,* pp. 331-341, 2006.

[9] P. Bungay, P. Morrison and D. Robert, "Principals of Quantitative Microdialysis," in *Handbook of Microdialysis Methods, Applications, and Clinical Aspects,* London, Academic Press, 2007, pp. 131-168.

[10] J. Stenken, "Methods and issues in microdialysis calibration," *Analitical Chemica Actica,* pp. 337-358, 1998.

[11] R. Schutte, S. Oshod and R. WM, "In vitro charectarazation of microdialysis sampling of macromolecules," *Anal Chem,* pp. 3777-3784, 2004.

[12] R. Schutte, S. Oshodi and W. Reichert, "In Vitro Characterization of Microdialysis

Sampling of Macromolecules," *Anylitical Chemistry,* vol. 76, no. 20, pp. 6058-6063, 2004.

[13] D. Crippensa, D. Camp and T. Robinson, "Basal extracellular dopamine in the nucleus accumbens during amphetamine withdrawal: a 'no net flux' microdialysis study," *Neuroscience Letters,* vol. 164, no. 1, pp. 145-148, 1993.

[14] K. Chen, "Evidence on extracellular dopamine level in rat striatum: implications for the validity of quantitative microdialysis," *Journal of Neurochemistry,* vol. 92, pp. 46-58, 2005.

[15] R. Cosford, A. Vinson and J. Kukoyi, "Quantitative microdialysis of serotonin and norepinephrine: pharmacological influences on in vivo extraction fraction," *Journal of Neuroscience,* vol. 68, pp. 39-47, 1996.

[16] L. Parsons, A. Smith and J. Justice, "dopamine is decreased in the rat nucleus accumbens during abstinence from chronic cocaine," *Journal of Neuroscience,* vol. 9, pp. 60-65, 1991.

[17] P. Lonnroth, P. Jannson and U. Smith, "A microdialysis method allowing characterization of intercellular water space in humans," *American Journal of Physiology,* vol. 257, pp. E228-E231, 1987.

[18] H. Yang, J. Peters and A. Michael, "Coupled effects of mass transfer and uptake kinetics on in vivo microdialysis of dopamine," *Journal of Neurochemistry,* vol. 71, pp. 684-692, 1998.

[19] T. Cremers, M. Vries and K. Huinink, "Quantitative microdialysis using modified ultraslow microdialysis: direct rapid and reliable determination of free brain concentrations with the MetaQuant technique," *Neuroscience Methods,* pp. 249-254, 2009.

[20] F. Adolf, "Poggendorff's Annalen," *Phiosophical Magazine,* vol. 10, pp. 30-39, 1855.

[21] A. Einstein, ""Über die von der molekularkinetischen Theorie der Wärme geforderte Bewegung von in ruhenden Flüssigkeiten suspendierten Teilchen" (in German).," *Annalen der Physik 322,* pp. 549-560, 1905.

[22] S. Lindsay, Introduction to Nanoscience, Oxford OUP, 2009.

[23] L. Dintenfass, "A new outlook on body fluid viscosity and cell function: concluding remarks and discussion.," *Biorheology,* pp. 611-616, 1990.

[24] S. Yedgar and N. Reisfeld, "Regulation of cell membrane function and secretion by extracellular fluid viscosity," *Biorheology. ,* pp. :581-588., 1990.

[25] Z. Mitchelle, "Composition and Viscosity of Interstitial Fluid of Rabbits," *Experimental*

Phisiology, vol. 80, pp. 203-207, 1995.

[26] P. Bungay, M. Paul and D. Robert, "Steady-State Theory for Quantitative Microdialysis of Solutes and Water in vivo and in vitro," *Life Sciences,* vol. 46, pp. 105-119, 1990.

[27] F. Wallgren, G. Amberg and R. Hickner, "A mathematical model for measuring blood flow in skelatal muscle with the microdialysis ethanol technique," *Journal of Applied Physilolgy,* vol. 659, no. 79, p. 648, 1995.

[28] J. Stenken, M. Southard, E. Topp and C. Lunte, "Examination of Microdialysis Sampling in a Well-Characterized," *Analytical Chemistry,* vol. 65, pp. 2324-2328, 1993.

[29] c. DD and S. e. JA, In vivo glucose sensors, Hoboken, NJ: John Wiley & Sons, 2010.

[30] J. Skyler, "Continuous Glucose Monitoring an overview of its development," *Diabetes Technol,* pp. 5-10, 2009.

[31] J. Stenken, D. Holunga, S. Decker and L. Sun, "Experimental and Theoretical Microdialysis Studies of in Situ Metabolism," *Analytical Biochemistry,* pp. 314-323, 2000.

[32] P. Bungay, R. Sumbria and B. Ulrick, "Unifying the mathematical modeling of in vivo and in vitro microdialysis," *Journal of Pharmaceutical and Biomedical Analysis,* vol. 55, pp. 54-63, 2011.

Appendices

Appendix A: Description of Research for Popular Publications:

You may or may not be aware of this, but cells are communicating with each other. Every time you move a muscle, every time you fight off the flu, every time your brain says, "I'm happy" cells are communicating.

There are a lot of people interested in listening in on these conversations and a lot of money being spent on it, including MS Micro EP student Cole Deaton under the direction of Dr. Julie Stenken at the University of Arkansas.

To interpret these communications researchers need to understand a three variable system. The three variables are concentrations of everything over time and space. It turns out this is easier said than done; mostly because in reality you can only observe at most two of these variables at once.

Microdialysis is a bioanalytical method that measures concentration as a function of time (holding space constant). The method consists of placing a diffusion based probe in the area of interest and flowing a liquid through it. Molecules diffuse across a semipermiable membrane into the flow and are carried off to collection. The problem is that the concentration collected is not the concentration that was present in the extracellular space.

Researchers have even instituted a term for it; they talk about the "relative recovery". Relative recovery is defined as what you collected divided by what was there times a hundred. There have been a lot of proposed answers to this problem since microdialysis's inception 30 years ago. The most satisfying of which are slowing the flow down through the membrane and placing affinity agents in the fluid flow.

What Mr. Deaton has done is created an answer that is better than all the existing answers. He accomplished this by looking at consequences to the current mathematical solutions to the fluid flow mass transfer problem for his particular situation. His answer is to recycle the flow back through the probe.

So, what makes his answer so cool? Well first of all it does what it is supposed to do. Isn't that nice when something does what it's supposed to.

Mr. Deaton concluded, "What I mean by that is that my method can produce relative recoveries of 100 percent. In addition to this, unlike the affinity agents, my answer can be applied to any analyte. Perhaps the coolest thing about my method is that in the future it will know when it's done collecting. What I mean by that is that the cyclic nature of my system and the asymptotic nature of the equations that govern it will lend themselves to self-automation."

Appendix B: Executive Summary of Newly Created Intellectual Property

The intellectual property (IP) that was created was the method of recycled flow microdialysis. This IP will not be able to be commercialized, because Dr. Julie Stenken publically disclosed the method, making any potential patent undefendable.

Appendix C: Potential Patent and Commercialization Aspects of listed Intellectual Property Items

C.1 Patentability of Intellectual Property (Could Each Item be Patented)

The intellectual property (IP) that was created was the method of recycled flow microdialysis.

C.2 Commercialization Prospects (Should Each Item Be Patented)

This IP will not be able to be commercialized, because Dr. Julie Stenken publically disclosed the method, making any potential patent undefendable.

C.3 Possible Prior Disclosure of IP

This IP was publically disclosed at Pittconn 2012.

Appendix D: Broader Impact of Research

The capability of microdialysis sampling to collect the molecules existing in the ECF of living tissue is significant because it makes possible the identification of bio markers for various disease states. [29] [30]. Microdialysis sampling can also be used to monitor localized metabolism in vivo and in vitro [31]. To understand the magnitude of the impact microdialysis sampling has had, on life science research consider a quote from CMA, the world leader in microdialysis probe sales "The first paper on Microdialysis was published in 1974. Since then, more than 13000, scientific papers have been published on the technique, among them some 2.000 clinical investigations [6].

E.2 Impact of Research Results on U.S. and Global Society

This research will indirectly affect the U.S. and global society. This research improves microdialysis sampling. Microdialysis sampling, arguably, affects the health and well being of the U.S. and global society.

E.3 Impact of Research Results on the Environment

This research method does not have any adverse environmental impact from the manufacture of the materials and devices.

Appendix F: Microsoft Project for MS MicroEP Degree Plan

Appendix G: Identification of All Software Used in Research and Thesis/Dissertation Generation

Computer #1:

Model Number: Dell Dimension 8300

Serial Number: 8654FG32

Location: PHYS134

Owner: Justin Cole Deaton

Software #1:

Name: Microsoft Office 2010

Purchased by: Justin Cole Deaton

Software #2:

Name: Maple 15

Purchased by: Justin Cole Deaton

Appendix H: All Publications Published, Submitted and Planned

Plagiarism Check

This dissertation/ thesis was submitted by {your name} to http://www.turnitin.com for plagiarism reviewed by the TurnItIn company's software. I examined the report on this dissertation that was returned by that plagiarism review site and attest that in my opinion the items highlighted by the software are incidental to common usage and are not plagiarized material.

_____

Ken Vickers

Director, MicroEP Graduate Program

_____

<Typed Name>

Dissertation Director